Magnetic and EPR study of $Zn_3Fe_4V_6O_{24}$

J. Typek[1,*], G. Zolnierkiewicz[1], N. Guskos[1,2], R. Szymczak[3], and A. Blonska-Tabero[4]

[1]Institute of Physics, Szczecin University of Technology, Al.Piastow 17, 70-310 Szczecin, Poland;
[2]Solid State Section, Department of Physics, University of Athens, Panepistimiopolis, 15 784 Zografos, Athens, Greece;
[3]Institute of Physics, Polish Academy of Sciences, Al. Lotnikow 32/46, 02-668 Warsaw, Poland;
[4]Department of Inorganic and Analytical Chemistry, Szczecin University of Technology, Al. Piastow 42, 70-065, Szczecin, Poland

Abstract

Polycrystalline samples of $Zn_3Fe_4V_6O_{24}$ prepared by solid-state reaction technique have been studied by magnetic and electron paramagnetic resonance (EPR) methods in the 2-300 K temperature range. Static magnetic susceptibility measurements showed the presence of strong antiferromagnetic interaction (Curie-Weiss temperature θ=-101 K) in the Fe^{3+} sublattice. The effective magnetic moment of a unit cell (about 11 μ_B for four iron ions) indicates on significant presence of antiferromagnetic correlations. At low temperature (3K and 6 K) clear indications of two spin-glass states were registered in the temperature dependence of susceptibility. Registered EPR spectra consisted of two components: a very broad line registered in high temperature range (above 15 K) and a narrow line below 15 K. The EPR amplitude of the broad component decreased with temperature decrease while the opposite trend was observed for the narrow line. On decreasing temperature from RT the broad line shifts slightly towards higher magnetic field and its linewidth increases. Large changes of g-factor and linewidth of this line are observed below 75 K. Temperature dependence of the EPR integral intensity of the broad line showed a marked anomaly at about 220 K in contrast to static magnetic susceptibility where no such irregularity was observed. The studied magnetic properties of $Zn_3Fe_4V_6O_{24}$ will be discussed in terms of an inherent magnetic inhomogeneity of this compound with competing magnetic interactions and spin clusters.

Introduction

Compounds in the multicomponent vanadates system M-Fe-V-O (M=Zn, Mg, Ni, Cu) attract much interest because of their complicated magnetic properties due, among others, to disorder in metal positions, oxygen deficiency and magnetic frustration [1-5]. They crystallize in the triclinic system and have an intricate structure with two metal ions subsystems. Magnetic frustration, frequently occurring in transition metal oxides, may lead to a highly degenerate ground state that obstructs long-range order. Well-known examples are spin glasses [6,7] and geometrically frustrated antiferromagnets, where all spin interactions can not be simultaneously minimized due to lattice geometry constraints [8-10]. The exceptional magnetic properties of the latter systems attract particular interest, aimed at the proper understanding of the cooperative paramagnetic state and the concurrent low-energy spectrum, while they have stimulated the search for materials exhibiting geometric frustration.

Recently, new compound $Zn_3Fe_4V_6O_{24}$ has been obtained as a product of a reaction between $FeVO_4$ and $Zn_3V_2O_8$. Neutron diffraction study has shown that it crystallizes in the triclinic space group P$\bar{1}$ and has a complicated structure with two metal ions subsystems [11]. Electron paramagnetic resonance (EPR) study of this compound at room temperature [12] and in high-temperature range [13] has shown its inherent magnetic inhomogeneity due to the presence of the antiferromagnetic spin clusters. EPR and thermogravimetric studies of $Zn_3Fe_4V_6O_{24}$ samples subjected to different thermal annealing processes have revealed that oxygen deficiency can introduce disorder and thus influence magnetic interactions in this multicomponent vanadate system [14]. Coexistence of two subsystems of magnetic iron(III) ions in multicomponent vanadates $M_3Fe_4V_6O_{24}$ (M(II)=Zn, Mg, Cu, Mn) has lead to the competition of magnetic interactions forming a frustrated system that prevents creation of a magnetically ordered state at high temperatures [15].

In this work, the magnetic properties of $Zn_3Fe_4V_6O_{24}$ are studied using static magnetization and electron paramagnetic resonance (EPR) measurements in a wide 2-300 K temperature range. An inhomogeneous ground state is derived, involving a frozen, spin-glass-like state at low temperatures and the presence of large AFM spin clusters, both pertinent to the existence of two magnetic subsystems and to disorder due to oxygen deficiency in this compound.

Experimental

Polycrystalline $Zn_3Fe_4V_6O_{24}$ samples were prepared by the solid-state reaction method using a stoichiometric mixture of the ZnO, V_2O_5 and Fe_2O_3 oxides, according to the reaction: 3 ZnO + 3 V_2O_5 + 2 Fe_2O_3 = $Zn_3Fe_4V_6O_{24}$. The obtained compound crystallized in the triclinic space group P$\bar{1}$ forming a brown-olive colour powder, with a melting point of 1123±5 K.

Static magnetization measurements were carried out both in the zero-field-cooled (ZFC) mode and field-cooled (FC) mode in 2-300 K temperature range on a MPMS-5 SQUID magnetometer. EPR measurements were carried out with a conventional X-band (ν = 9.43 GHz) Bruker E500 spectrometer, with 100 kHz magnetic field modulations. The EPR thermal studies were performed in 4-300 K temperature range using an Oxford helium-flow cryostat.

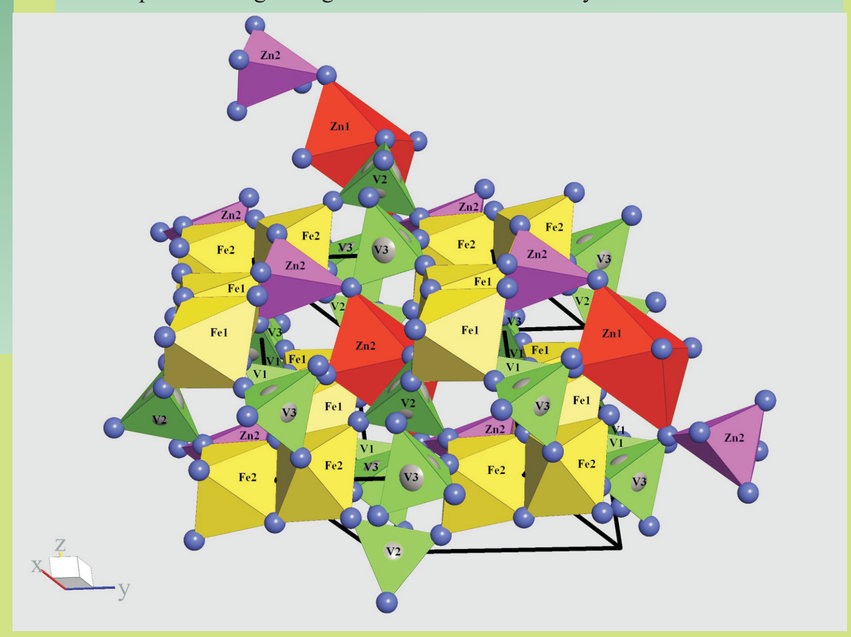

Figure 1. Schematic structure of $Zn_3Fe_4V_6O_{24}$.

Results and discussion

The crystal structure of $Zn_3Fe_4V_6O_{24}$ is build up from ZnO_6 polyhedra, ZnO_5 trigonal bipyramids, FeO_6 octahedra and isolated VO_4 tetrahedra **(Fig. 1)**. The linkage of the octahedral and trigonal bipyramids could be seen in **Fig. 1**. Fe_2O_{10} octahedral dimers alternate with ZnO_5 bipyramids to form edge-sharing chains. The ZnO_6 octahedra are located between the chains and share corners with both the ZnO_5 and Fe_2O_{10} units. There are two crystallographic sites for Fe ions: Fe(1) and Fe(2) with two formula units in the unit cell. The distance between neighbouring Fe(1) ions (3.192 Å) is longer than between Fe(2) ions (3.117 Å) [11]. Although Fe(1) and Fe(2) octahedra form edge-sharing dimeric clusters, their environment of the vanadium tetrahedral VO_4 is different. The $Fe(2)_2O_{10}$ octahedral dimers are surrounded by ten isolated VO_4 tetrahedra, sharing each one corner with the Fe(2) dimer, and therefore they form a $Fe(2)_2O_{10}$ unit. Only eight VO_4 tetrahedra build up $Fe(1)_2O_{10}$ unit. They are linked to Fe(1) dimer, since two of them $V(2)O_4$ share two vertices, instead of one, with the dimer.

Figure 2 shows the temperature dependence of the magnetic susceptibility χ and the inverse susceptibility χ^{-1}, derived from static magnetization measurements in the ZFC mode as M_{ZFC}/H. The Curie-Weiss behaviour is evident in the high-temperature range. At T >70 K, the Curie-Weiss fit to the $\chi^{-1}(T)$ data yields an effective moment of 11.01(5) μ_B per formula unit for H=50 Oe and 10.89 μ_B for H=6000 Oe, and a negative Curie-Weiss temperature $\Theta = -101.4(1)$ K and $\Theta = -100.7(1)$ K, respectively. The obtained value of an effective magnetic moment for one iron ion ~2.7 μ_B differs significantly from the high-spin only value of Fe^{3+} ion (s=5/2, μ=5.92 μ_B). The value of the Weiss temperature suggests substantial antiferromagnetic interactions, the strongest most likely occurring within the $Fe(1)_2O_{10}$ octahedral dimer with the shortest internuclear distance [Fe(1)-Fe(1)]. Such type of coupling complies with the Goodenough-Kanamori rules predicting predominantly antiferromagnetic superexchange pathways for the $d^5 - d^5$ pair interaction [16].

In the 70-25 K temperature range a slight upturn is observed in χ^{-1}. However, at T < 10 K, the dc susceptibility χ exhibits a very interesting behaviour. At T_{f1}=6 K a weak maximum in $\chi(T)$ is observed in ZFC and FC mode, while another maximum is registered at T_{f2}=3 K only in ZFC mode **(Fig. 3)**, suggestive of a spin-glass-like transition. This two temperatures, T_{f1} and T_{f2} could be regarded as freezing temperatures to the spin glass state in two magnetic sublattices Fe(1) and Fe(2). Comparison of the Curie-Weiss temperature that sets up the mean-field energy scale for the antiferromagnetic pairwise coupling of Fe^{3+} spins (Θ≈100 K) and the freezing temperature T_f yields the ratio $r=\Theta/T_f$≈20, suggesting a significant spin frustration as well as appreciable AFM correlations in the paramagnetic phase. It would be tempting to associate 6 K maximum in χ(T) with the antiferromagnetic Neel temperature T_N, but the measurements of $M(H)$ below that temperature **(Fig. 4)** did not indicate on the presence of a long range magnetic order in $Zn_3Fe_4V_6O_{24}$ at T=5 K.

Figure 5 shows representative EPR spectra of $Zn_3Fe_4V_6O_{24}$ at different temperatures. A single, broad resonance line at $g \approx 2.0$ dominates the spectra in a wide temperature range from 10 to 300 K. Below 10 K a narrow line begins to gain intensity with temperature decrease. It could be attributed to paramagnetic impurities strongly coupled to the lattice. To evaluate the temperature variation of the EPR parameters of the broad line, the derivative spectra were fitted to a full Lorentz line comprising the tail of the resonance absorption at negative field, a consequence of the linearly polarized rf field that is important when the width becomes comparable to the resonance field. **Figure 6** summarizes the temperature dependence of the linewidth ΔH_{pp} (determined as a peak-to-peak value of the first derivative of the absorption curve) and the effective g-factor. Such a temperature variation of linewidth ΔH and g-factor is frequently observed near magnetic phase transitions for ordinary antiferromagnets [17] or spin-glasses [18], due to the slowing down of spin fluctuations and the growth of internal fields. The linewidth increases sharply with lowering temperature, and below 20 K is so broad that it is difficult to estimate credibly its value. The EPR linewidth variation with temperature could be analyzed using two different expressions. If the thermal change of linewidth is attributed to the spin-glass to paramagnetic transition at temperature T_f, the following expression is valid [19]

$$\Delta B_{pp} = \Delta B_0 + A \cdot \left(\frac{T_f}{T - T_f} \right)^{\alpha} \qquad (1)$$

where ΔB_0 is the temperature independent part of linewidth, A is a constant, and α is the critical exponent. The **solid line in Fig. 6** represents the best fit of **equation (1)** to the experimental data with ΔB_0=110(2) mT, T_f=10.2(8) K, α=1.07(5). The second expression is based on assumption that the broadening is due the spatial inhomogeneity (e.g. as a result of oxygen deficiency) resulting in an effective clustering of iron ions [20]:

$$\Delta B_{pp} = \Delta B_0 + \Gamma \cdot \exp\left(-T / T_0\right) \qquad (2)$$

In (2) Γ is a constant T_0 corresponds to the potential barrier separating two neighbouring ground states of the disordered spin system. The **dotted line in Fig. 6** represents the best fit of **equation (2)** to the experimental data with ΔB_0=137(4) mT, and T_0=16(1) K. Comparing the fitted results it should be remarked that the first model better describes the linewidth variation on temperature. The calculated value of the freezing temperature T_f is higher than that obtained from static magnetization measurements. This discrepancy might be explained by application of large static magnetic field (~3300 Oe) in EPR measurements that shifts T_f to higher temperatures. The obtained value of the critical exponent α is very close to 1 what indicates on a 3D character of magnetism in this compound.

Figure 7 presents the temperature dependence of the integral intensity, reciprocal of integral intensity, and the product of integral intensity and temperature. The EPR integral intensity, I_{int}, is calculated as the product of signal amplitude and the square of the linewidth. It is suppose to be proportional to the magnetic susceptibility of the spins taking part in the resonance. On the other hand, the product $I_{int} \cdot T$ is proportional to the effective magnetic moment of the spins participating in EPR. The temperature dependence of I_{int} displays a very peculiar behaviour. In the high-temperature range it reaches minimum at ~195 K and increases with temperature increase up to ~230 K. Upon further heating I_{int} decreases again. The high temperature minimum of I_{int} was registered also for other compounds in $M_3Fe_4V_6O_{24}$ family (M=Mg, Mn, Cu) [15]. This seems to be a sample dependent phenomenon that could be explained as a result of strong competition of magnetic interactions. The level of sample oxygen deficiency, influencing the degree of disorder, appears to play a leading role in this behaviour. It is worth noting that the magnetic inhomogeneity may be further promoted by the presence of oxygen deficiency and a small fraction of magnetic vanadium spins (e.g. V^{4+} with spin S = 1/2) that may disrupt or enhance the exchange coupling of Fe^{3+} moments.

As the effective magnetic moment decreases with temperature decrease **(Fig. 7. lower panel)** the leading interaction is of antiferromagnetic type. Below 170 K $I_{int}(T)$ shows roughly the Curie-Weiss behaviour, but in comparison with $\chi(T)$ obtained in static magnetization measurements **(Fig. 2)** the calculated antiferromagnetic Curie-Weiss temperature (Θ≈-25 K is significantly reduced. To explain the difference in behaviour of $I_{int}(T)$ and $\chi(T)$ in high temperature the concept of dynamical spin clusters should be introduced. These antiferromagnetic spin clusters of short-range ordered spins only exist on the time scale of the microwave radiation used in EPR technique (τ=1/ν≈10^{-10} s) and thus could be registered only by this method. For static measurements only separated spin are seen.

In the antiferromagnetic temperature range of the $\chi_{EPR} \approx T$ product (i.e. below 170 K) the effective resonance field increases sharply (g-factor decreases) with the temperature decrease **(Fig. 6)**. This increase could be attributed to the appearance of local fields created by antiferromagnetically correlated spins. These fields add to the applied eternal field, changing the resonance condition. Assuming that there are antiferromagnetically correlated spins between ferromagnetic layers, the effective resonance field B_r could be approximated by the equation [21]:

$$B_r(T) = C_1 + \frac{C_2}{T \cdot \exp\left(\frac{C_3}{T}\right)} \qquad (3)$$

where C_1, C_2 and C_3 are constants and C_3 contains, among others, the antiferromagnetic exchange coupling between layers of spins. Thus the temperature dependence of g-factor should be described by the function

$$g(T) = C_0 \left(C_1 + \frac{C_2}{T \cdot \exp\left(\frac{C_3}{T}\right)} \right)^{-1} \qquad (4)$$

where $C_0 = h\nu/\beta$. The **solid line in Fig. 6** is the best fit to Eq. (4).

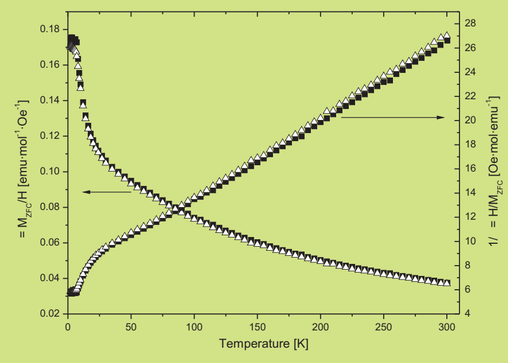

Figure 2. Temperature dependence of the magnetic susceptibility χ (left axis) and the inverse susceptibility χ^{-1} (right axis), derived from static magnetization measurements in the ZFC mode as M_{ZFC}/H for H=50 Oe (filled squares) and H=6000 Oe (open triangles).

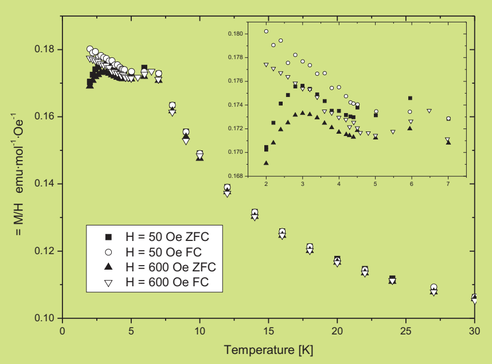

Figure 3. Temperature dependence of the magnetic susceptibility χ in the low temperature range. The inset shows this behaviour in detail in the 2-7 K range.

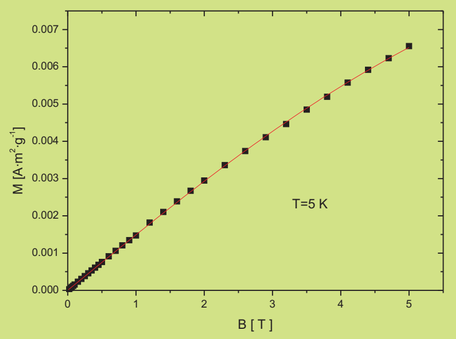

Figure 4. Magnetic field dependence of magnetisation M at T=5 K. The solid line is the least-square fitting to the Brillouin function.

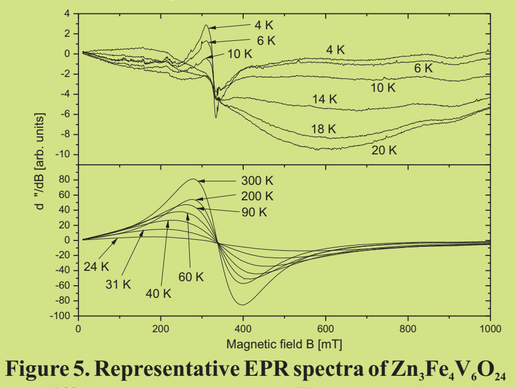

Figure 5. Representative EPR spectra of $Zn_3Fe_4V_6O_{24}$ at different temperatures. Upper panel – low temperature range (4-20 K), lower panel – high temperature range (24-300 K).

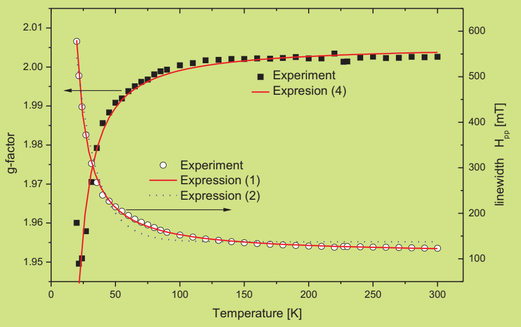

Figure 6. Temperature dependence of the effective g-factor (left axis) and the peak-to-peak linewidth (right axis).

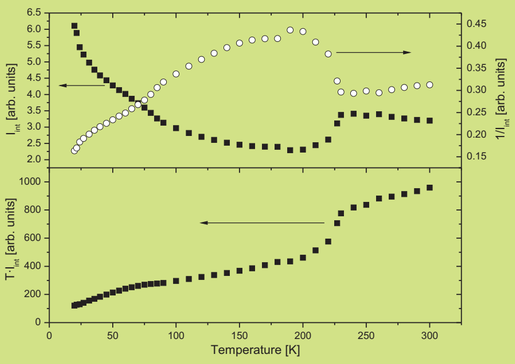

Figure 7. Temperature dependence of the EPR integral intensity, I_{int}, (upper panel, left axis), reciprocal of integral intensity, I_{int}^{-1}, (upper panel, right axis), and the product $I_{int} \cdot T$ (lower panel).

Conclusions

In conclusion, dc magnetization and EPR measurements on the recently synthesized ternary vanadate $Zn_3Fe_4V_6O_{24}$ provide experimental evidence for the presence of significant magnetic frustration due to the oxygen deficiency and the occurrence of two magnetic sublattices. In particular, the dc magnetic susceptibility indicates low-temperature spin freezing in two magnetic sublattices at T_f = 3 K and 6 K, and the existence of strong antiferromagnetic correlations appearing from high temperatures. EPR studies confirmed the presence of antiferromagnetic interactions and most remarkably revealed the presence of another magnetic contribution peaking at ~230 K and not visible to static magnetization measurements.

Corresponding author: (J. Typek), e-mail: typjan@ps.pl